



TITLE:

# Direct Observation of Disorders of Molecular Stacking in Pt-Phthalocyanine Epitaxial Film

AUTHOR(S):

Yase, Kiyoshi; Kobayashi, Takashi; Uyeda, Natsu

---

CITATION:

Yase, Kiyoshi ...[et al]. Direct Observation of Disorders of Molecular Stacking in Pt-Phthalocyanine Epitaxial Film. Bulletin of the Institute for Chemical Research, Kyoto University 1986, 63(5-6): 383-392

ISSUE DATE:

1986-03-03

URL:

<http://hdl.handle.net/2433/77129>

RIGHT:

## Direct Observation of Disorders of Molecular Stacking in Pt-Phthalocyanine Epitaxial Film

Kiyoshi YASE\*, Takashi KOBAYASHI and Natsu UYEDA

*Received January 7, 1986*

The epitaxial films of Pt-phthalocyanine (Pt-Phc) formed on a mica surface have been investigated by high resolution electron microscopy. The molecular shapes were directly detected as the stripes in the images. Though the molecular stacking in the column is identical with those in the  $\alpha$ -form Pt-Phc crystal, the arrangement of the columns varies in local as if each small area of the crystal assumes a different polymorph. The plural modes of the arrangement co-exist in one crystallite. The elemental stacking modes of the columns have been derived and the electron diffraction pattern of the film can be explained by this model.

KEY WORDS: Thin organic film/ Phthalocyanine/ Polymorph/ Disorder/ Stacking fault/ Epitaxial film/

### INTRODUCTION

Metal phthalocyanines (M-Phcs; M=Pt, Cu, Ni, Fe, H<sub>2</sub>, etc.) vacuum deposited on a single crystal surface, grow epitaxially under appropriate conditions. Their structures have been studied by electron diffraction<sup>1,2)</sup>. They have concluded that M-Phc grown on mica surface had an isomorphic structure, regardless of the species of the central metals, with the  $\alpha$ -form Pt-Phc crystal. The space group, cell constants and atomic parameters of the single crystal were determined by Brown from the X-ray data<sup>3)</sup>. According to his results, the structure of the  $\alpha$ -form Pt-Phc belongs to a monoclinic system of the space group C2/n and has the following unit cell constants;  $a=26.46$ ,  $b=3.76$ ,  $c=24.28$  Å and  $\beta=93.53^\circ$ . The projections of the molecules along the main crystal axes are reproduced in Figs. 1 (a,b,c). The molecules stand in a line to form the molecular columns along the b-axis. The angle between the b-axis and the normal of the molecular plane is  $25.6^\circ$ . The distance between the mean planes of two adjacent molecules is 3.45 Å.

The present authors have, however, revealed by high resolution electron microscopy (HREM) that there are several different structures in the evaporated thin films of Zn-Phc grown on amorphous carbon films<sup>4)</sup>. The crystal structure of divalent metal phthalocyanines can be characterized by the existence of molecular columns, in which planar molecules are piled up on one another. The crystal structure of planar

八瀬清志, 小林隆史, 植田 夏: Laboratory of Crystal and Powder Chemistry, Institute for Chemical Research, Kyoto University, Uji, Kyoto-Fu 611.

\* Present Address; Faculty of Applied Biological Science, Hiroshima University, Fukuyama, Hiroshima 720.

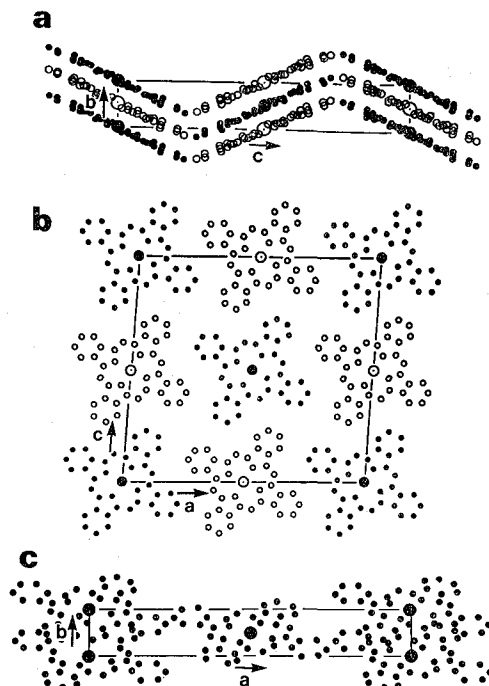


Fig. 1. The projections of the  $\alpha$ -form Pt-Phc crystal along the main crystal axis; (a) a, (b) b and (c) c-axes projection. The crystallographic equivalent positions are followings;  $\pm(x, y, z)$ ,  $\pm(x+1/2, -y, z+1/2)$ ,  $\pm(x+1/2, y+1/2, z)$  and  $\pm(x, -y+1/2, z+1/2)$ . The (001) projection shows only the molecules whose centers locate at the unit cell origins.

molecules can be represented by the following two characteristics. One is the structure of the column, that is, the molecular orientation in the column. The other is the arrangement of the columns in the crystal as a whole. These characteristics can be determined by the direct observation of molecular images in projections of the molecular columns. The column axis is taken in general as the crystallographic b-axis. The structure images of Zn-Phc projected along the column axis and the disorders in the crystals have been discussed in detail<sup>5)</sup>.

In this work, the direct observation of the molecular images forming the columns and the arrangements of the columns has been attempted and the three dimensional structure models have been established for the thin epitaxial films of Pt-Phc.

#### EXPERIMENTAL PROCEDURES

The Pt-Phc powder was used after the purification by repeated sublimations in nitrogen gas-flow. After mica cleaved in air was degassed at 200 °C for 2 hours in a vacuum of  $1 \times 10^{-5}$  Pa, Pt-Phc was sublimed on the substrate kept at the same temperature. The film thickness was monitored by a quartz crystal micro-balance

during the evaporation and controlled to be 10 nm. The film was reinforced with amorphous carbon of a few nm in thickness. The specimen was stripped from the substrate by the immersion into distilled water and was transferred on microgrids coated with gold. The gold on microgrid was used as the standard for the calibration of camera length in electron diffraction and of magnification in HREM. The electron microscope used was JEOL JEM-200CX (acceleration voltage; 200 KV, point-to-point resolution; 2.0 Å) equipped with a high resolution pole-piece for objective lens and a minimum dose system, which was developed to perform HREM with radiation sensitive specimens<sup>6)</sup>.

## RESULTS AND DISCUSSION

### (1) Electron diffraction pattern

An electron micrograph of the evaporated film of Pt-Phc grown on a mica surface is reproduced in Fig. 2(a), which shows that the thin film is composed of many

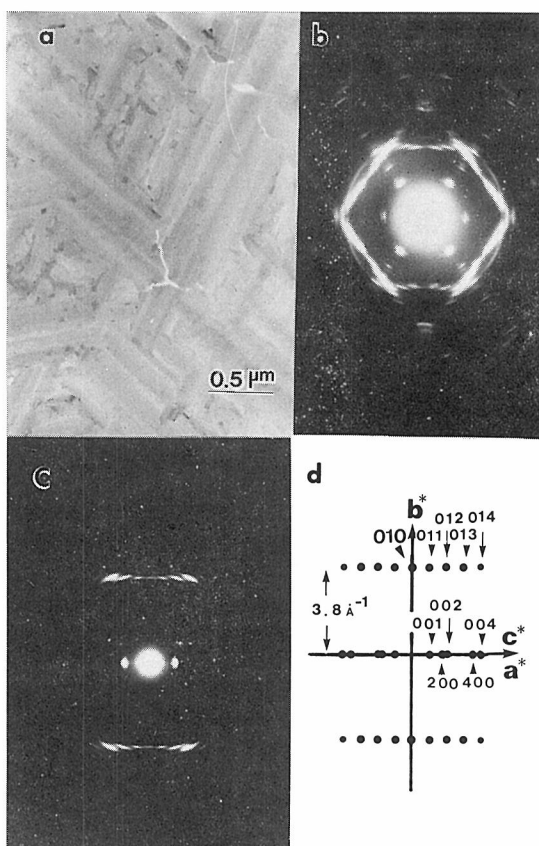


Fig. 2. (a) The electron micrograph of the Pt-Phc film. (b) The high resolution electron diffraction (HRED) pattern and (c) the selected area electron diffraction (SAED) pattern obtained from sub- $\mu\text{m}$  region. (d) The schematic illustration of the SAED pattern of (c).

crystallites elongated into three directions reflecting the symmetry of the substrate structure. In each direction, the crystals have domain sizes of a few  $\mu\text{m}$ . The high resolution electron diffraction (HRED) and a selected area electron diffraction (SAED) patterns are shown in Figs. 2(b, c) respectively. In Fig. 2(b), three equivalent fiber patterns are superimposed on each other showing six-fold symmetry. The SAED shows only one elemental pattern because the contributed area to the diffraction pattern is so small in the latter case that one single crystal can be selected. The SAED shown in Fig. 2(c) also exhibits a texture pattern whose fiber period is 3.80 Å. On the equator two series of diffraction spots can be observed. They correspond to the interplanar spacing of 24.2 (or 12.1) Å and 13.2 Å. On the other hand, the first layer shows only a spot array corresponding to 24.2 Å lattice intervals. The following two points should be emphasized here. One is the presence of a diffraction spot at the center of the first layer line. The second is the fact that the series of diffraction spots coming from the 13.2 Å lattice plane can not be observed on the first layer though they appear on the equator.

The lattice dimensions obtained from the electron diffraction shown above coincide well with those determined by Brown. On the basis of this fact, we tentatively assume the epitaxial film of Pt-Phc on mica to be the  $\alpha$ -form. Then the fiber axis is identified to be the b-axis and the diffraction spots on the first layer can be indexed as  $(01\ell)$  where  $\ell=0, \pm 1, \pm 2$ , etc., while those on the equator are  $(h00)$  and  $(00\ell)$  where  $h$  is even numbers and  $\ell$  is all natural numbers.

The results of crystal structure analysis of the  $\alpha$ -form Pt-Phc refined by Brown have shown that the crystal has a monoclinic lattice belonging to the space group of  $C2/n$  as introduced above (Fig. 1). If the epitaxial film has the same structure with the  $\alpha$ -form, its diffraction pattern ought to satisfy the following extinction rules<sup>7)</sup>;  $hk0$  with  $h+k=2n$ ,  $0k\ell$  with  $k=2n$  are possible reflections. Therefore, the  $0k\ell$  reciprocal lattice plane lacks the lattice points having odd  $k$  values and the  $hk0$  plane shows the alternate arrangement of the reflection spots under the condition of  $h+k=2n$ . These situations are shown schematically in Fig. 3.

The electron diffraction pattern obtained from the present specimen is shown in Fig. 2(c) with its schematic representation (Fig. 2(d)). The observed pattern resembles the illustration shown in Fig. 3 which are derived from the  $\alpha$ -form structure. Though the unit cell dimensions agree well, the extinction rules are quite different from each other.

In the two dimensional projections, the crystal structure can be explained by the use of the plane group. The plane groups of the a and c-axes projections, which include the b-axis of the  $\alpha$ -form structure, are  $p2mg$  ( $a'=c$  (24.2Å),  $b'=b/2$  (1.90Å)) and  $c2mm$  ( $a'=a$  (26.4Å),  $b'=b$  (3.80Å)), respectively. Here  $a'$  and  $b'$  denote the unit cell constants of the two dimensional lattices. In the a-axis projection,  $b'$  is equal to one half of  $b$ . The symmetry operation of the  $C2/n$  space group demands the molecule to be located at  $(x+1/2, y+1/2, z)$ . The schematic diffraction patterns are shown in Figs. 3(a, b), where the diffraction intensities are not taken into consideration. The a-axis projection of the  $\alpha$ -form has no reflections on the  $k=\pm 1$  layer and the c-axis projection lacks the  $010$  reflection. In both projections, the reflec-

tions on the equator ( $k=0$ ) with the odd indexes are extinguished. In other words, the first layer ( $k=\pm 1$ ) of a-axis projection and 010 reflection of c-axis projection are forbidden in the  $\alpha$ -form structure. However, the SAED patterns (Figs. 2(c,d)) show the existence of these diffraction spots. These facts reveal that the epitaxial film has the different symmetry or structure from the  $\alpha$ -form crystal. The thin film, therefore, is expected to be composed of crystallites having several different structures.

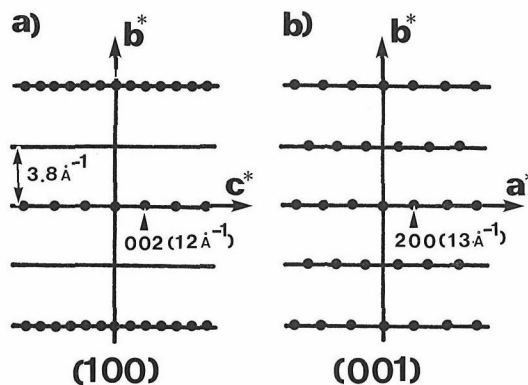


Fig. 3. The expected diffraction patterns of the  $\alpha$ -form Pt-Phc crystal structure along the a-axis (a) and c-axis (b), where the reflection intensities are not considered.

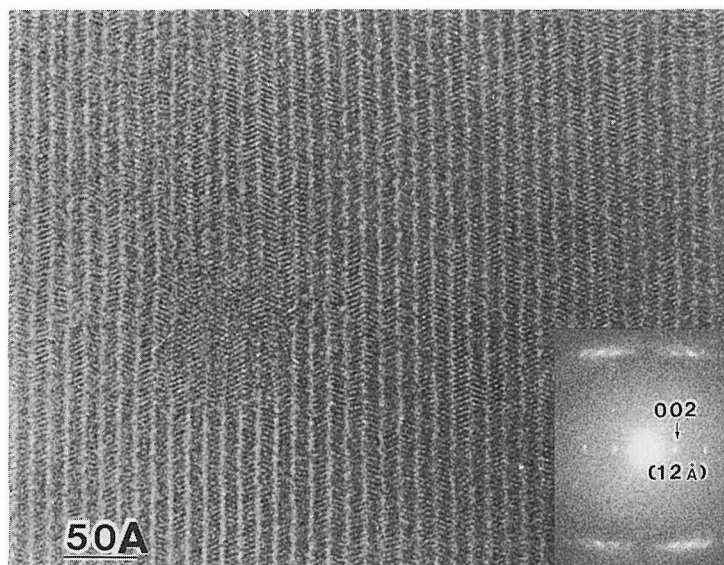


Fig. 4. The high resolution electron micrograph and its optical transform. The lattice fringes show the molecular columns with the spacing of 12 Å. The detail in the column is represented in Fig. 6.

The detailed discussion will be described in the next section.

## (2) HREM image and its computer simulation

A HREM image of Pt-Phc thin film showed lattice fringes with  $12.1 \text{ \AA}$  spacing, corresponding to (002) planes. In the fringes, many stripes are observed as shown in Fig. 4, with the optical transform by means of laser beam which coincides well with the SAED pattern (Fig. 2(c)). Each stripe corresponds to the image of the Pt-Phc molecule viewed along the molecular plane.

It can be observed that the several modes of molecular packing co-exist in the micrograph. They are separately enlarged and represented in Figs. 5(a, b, c, d) with respective computer simulations. The stripes are piled up in the columns with the interval of  $3.8 \text{ \AA}$ , which corresponds to the fiber period and therefore the unit cell dimension along the b-axis. The stripes tilt to make an angle of  $63^\circ$  with the column axis. Fig. 5(a) looks like the image of the a-axis projection shown in Fig. 1(a),

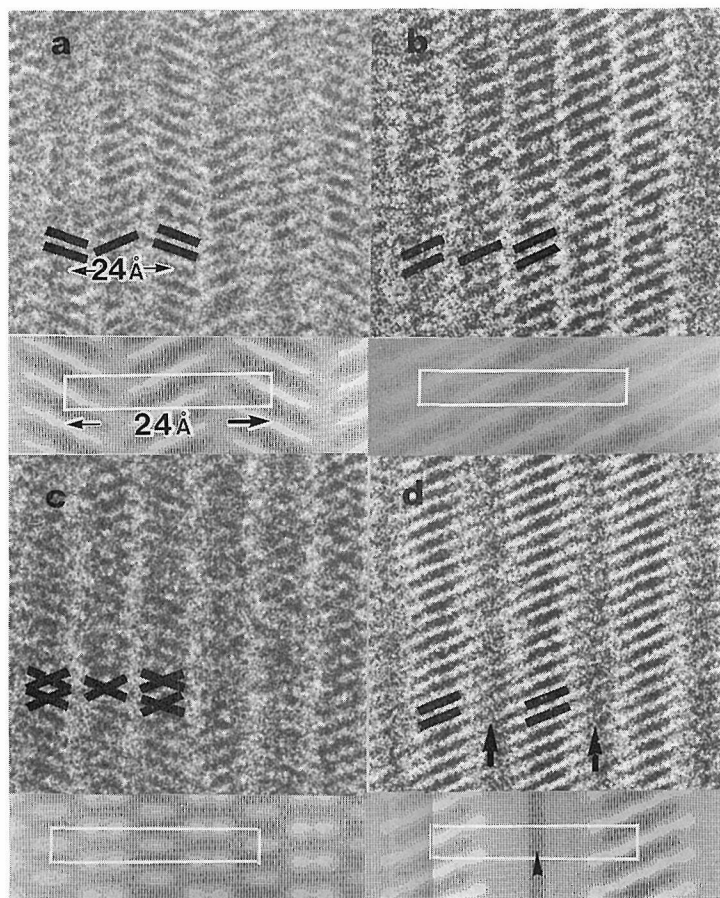


Fig. 5. The typical molecular arrangements in columns with computer simulations. The unit cell is indicated by the white rectangle in the picture.

where the interval of the stripes is  $1.9 \text{ \AA}$ . However, the observed molecular interval is  $3.8 \text{ \AA}$ . This shows that the molecules located at  $(x+1/2, y+1/2, z)$  do not exist in the observed images. The EM used in the present work has the theoretical point-to-point resolution of  $2.0 \text{ \AA}$ . The HREM images of a-axis projection of the  $\alpha$ -form, therefore, should show only lattice fringes with  $12 \text{ \AA}$  spacing and no individual molecules in the fringes because of the lack of the resolution. The imaging of the molecules projected on the plane including the b-axis needs interference of the reflections with the indexes of  $k=0$  and  $k=\pm 1$  of the  $\alpha$ -form structure. In spite of the fact that the a-axis projection has no reflections with  $k=\pm 1$  ( $3.8 \text{ \AA}^{-1}$ ), as shown in Fig. 3(a), the  $12 \text{ \AA}$  fringes reveal clearly the molecular images as stripes with the interval of  $3.8 \text{ \AA}$ . This fact also indicates the existence of some other kinds of structures in the epitaxial films.

The fact that the molecular images appeared in various ways different from those expected for the  $\alpha$ -form can be confirmed by computer simulations. When the resolution is better than  $1.9 \text{ \AA}$ , molecular images of the  $\alpha$ -form where the molecules stack showing the  $1.9 \text{ \AA}$  spacing in projection can be resolved at least to an extent to show the periodicity, as shown in Fig. 6(a). If the resolution is lower

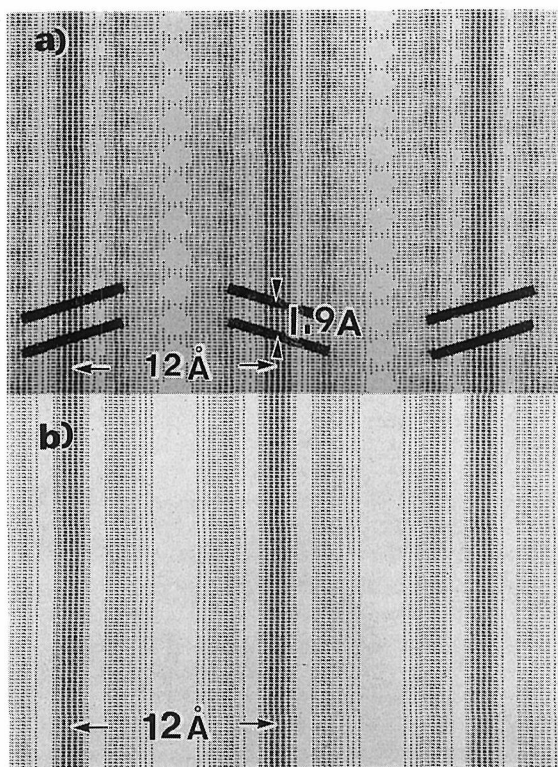


Fig. 6. The computer simulations of the  $\alpha$ -form Pt-Phc single crystal projected along the a-axis with the different resolutions of  $1.9 \text{ \AA}$  (a) and  $2.5 \text{ \AA}$  (b).



than  $1.9 \text{ \AA}$ , the electron micrograph shows only the  $12 \text{ \AA}$  fringes, as shown in the simulated image in Fig. 6(b). On the other hand, the simulation using the parameters of the structure model shown in Fig. 7(a) derived from the observed HREM image (Fig. 5(a)), agreed well with the image. The columns denoted by **A** or **B** are designated in the next section as well as the **A'** or **B'**. Similarly, the other HREM images shown in Figs. 5(b,c,d) are also reconstructed by the computer simulation for the crystal models (Figs. 7(b,c,d)) for each image. These models derived from the HREM images of Fig. 5 are exhibited with the corresponding plane groups and the possible reflections obeying the extinction rules. These plane groups are  $p2gg$ ,  $c2$ ,  $c2mm$  and  $p2$  with the cell dimensions of  $a'=c(24.2 \text{ \AA})$  and  $b'=b(3.80 \text{ \AA})$  for model (a, b, c, d), respectively. The 010 reflection is possible when the crystal takes the model (d) with the plane group of  $p2$ . The molecular arrangements in every HREM

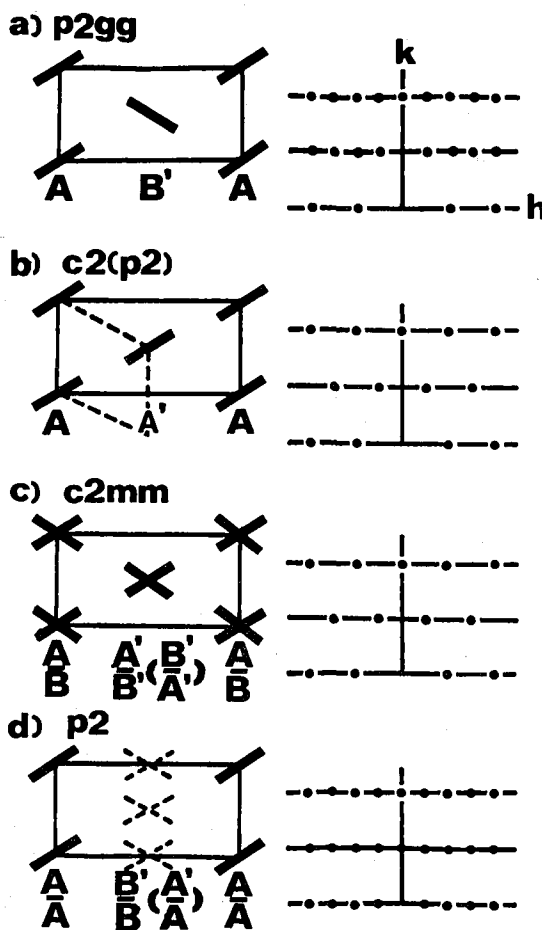


Fig. 7. The models of molecular arrangements shown in Fig. 5 and the schematic diffraction patterns with the index of the plane group.

images thus differ clearly from those in the  $\alpha$ -form structure. The real thin film consists of many domains with different structures and sizes of a few hundreds Å as shown in Fig. 5. Both of the HRED and SAED methods can not select one such a small domain individually. The SAED patterns shown in Fig. 2(c) is regarded as the superposition of the four patterns deduced from the model (a) to (d).

The SAED from the epitaxial films includes the diffraction spots corresponding to the 13 Å lattice spacing. However, no detail can be observed in the lattice fringes. This is partly due to the lack in the resolution of the images and may partly be due to the more complex molecular orientations than those described above.

### (3) Structure of epitaxial film

As so far described, the crystalline films of Pt-Phc epitaxially grown on a cleaved mica surface are composed of some crystallites in which molecular columns arrange in various modes of orientations. These molecular columns of Pt-Phc have the same structure, i.e., the molecular stacking in the column are identical for all columns in the film. Fig. 8(a) shows a stacking of the Pt-Phc molecules forming the column. The columns located with this orientation on the substrate are designated here the column **A**. If the columns take another orientation related to the column **A** with a mirror symmetry, they are named as column **B**. When these columns **A** or **B** shift a half period along the column axis in the same plane relative to the adjacent one, they are denoted as **A'** or **B'**, respectively. With these notations, all of the structures found in the epitaxial film can be represented. The structures displayed in the

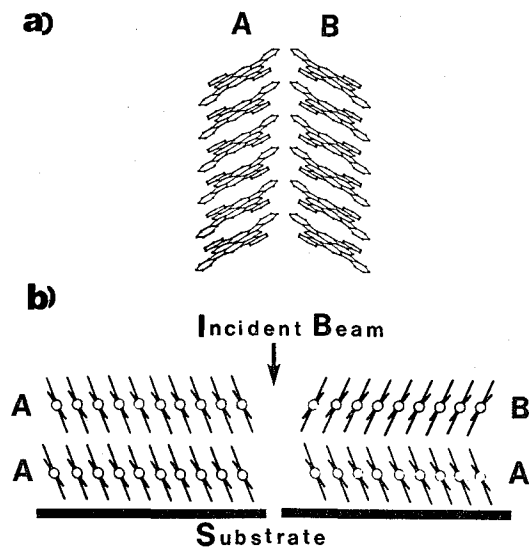


Fig. 8. (a) The arrangements of different molecular columns in the crystalline film. The columns of **A** and **B** are related to each other by the mirror plane. (b) The column stacking normal to the film surface.

HREM images shown in Figs. 5(a) and (b) are expressed in  $[\text{AB}'\text{AB}']$  and  $[\text{AA}'\text{AA}']$  or  $[\text{BB}'\text{BB}']$ , respectively. Here one must notice the fact that the electron micrograph is a projection of a specimen having a three dimensional structure. Many columns pile up on another in the crystal along the projection axis. Therefore, the images of many columns are superimposed on each other. When the column **A** stacks on **B**, the projection becomes cross hatched images. This situation can be seen in the HREM image shown in Fig. 5(c). However, when the column images of **A** and **A'** or **B** and **B'** are overlapped, the molecular images of one column (**A** or **B**) are inserted in the gaps of the other images of the molecular column **A'** or **B'**. As the result, molecules appear to arrange as if they stack in the column with an interval of a half period of the original one. In the present case, the original period is 3.8 Å and then the half period is 1.9 Å which can not be resolved by the EM used here. The column image in such a case becomes a line having no fine structure in it. Fig. 5(d) is the alternate arrangement of the images of column **A** and the fringes without fine structures, as indicated by arrows.

The following conclusions about the structure of the epitaxial film of Pt-Phc are derived from the fact mentioned above.

- (a) The molecular stacking in the column is identical with that of in the  $\alpha$ -form.
- (b) The arrangement of the column varies in local as if each small area of the crystal assumes a different polymorph.
- (c) The plural modes of the arrangement co-exist in one crystallite.
- (d) The variation of stacking of the molecular columns occurs not only in film plane but also along the projection axis.
- (e) The stacking modes of the columns result in the appearance of plural numbers of structures in one epitaxial film differing from the  $\alpha$ -form.

Finally, it must be pointed out that these structures can not be detected by any other methods like electron or X-ray diffraction except the direct observation of molecular images by HREM.

## REFERENCES

- 1) M. Ashida, N. Uyeda and E. Suito, *Bull. Chem. Soc. Japan*, **39**, 2616 (1966).
- 2) M. Ashida, *Bull. Chem. Soc. Japan*, **39**, 2625 and 2632 (1968).
- 3) C. J. Brown, *J. Chem. Soc.*, (A) 2494 (1968).
- 4) T. Kobayashi, Y. Fujiyoshi, F. Iwatsu and N. Uyeda, *Acta Cryst.* **A37**, 692 (1981) and T. Kobayashi, Y. Fujiyoshi and N. Uyeda **A38**, 356 (1982).
- 5) T. Kobayashi, Y. Fujiyoshi, and N. Uyeda, *J. Cryst. Growth*, **65**, 511 (1982).
- 6) Y. Fujiyoshi, T. Kobayashi, K. Ishizuka, N. Uyeda, Y. Ishida and Y. Harada, *Ultra-microscopy*, **5**, 459 (1980).
- 7) "International Tables for X-ray Crystallography Vol. A," The Kynoch Press, (1983).